



---

*Research article*

## **Effects of a protection zone in a reaction-advection-diffusion model with strong Allee effect**

**Dedicated to Professor Yang Kuang on the occasion of his 60th birthday**

**Davis Henderson<sup>1</sup> and Bingtuan Li<sup>2,\*</sup>**

<sup>1</sup> Department of Mathematics, Indiana University, Bloomington, IN 47404, USA

<sup>2</sup> Department of Mathematics, University of Louisville, Louisville, KY 40292, USA

\* **Correspondence:** Email: [bing.li@louisville.edu](mailto:bing.li@louisville.edu).

**Abstract:** We consider a reaction-advection-diffusion equation that models a population in a bounded habitat with a strong Allee effect and a protection zone. We assume that the population growth function exhibits the strong Allee effect and has a positive integral within the protection zone (indicating population persistence) and a negative integral in the surrounding patches (indicating population decay). We prove that the existence of positive steady-state solutions to this system depends on the length of the protection zone. It is demonstrated that there exists a threshold value  $H^*$  such that, for a protection zone of size  $H^*$ , there exists one positive steady-state solution and, for a larger protection zone, there exist multiple positive steady-state solutions. For smaller protection zones, we prove there exists no positive steady-state solution. The dynamics of the equation are further examined via numerical simulations.

**Keywords:** reaction-advection-diffusion equation; protection zone; Allee effect; steady-state solution; persistence

---

### **1. Introduction**

In this paper, we are concerned with the reaction-advection-diffusion model

$$u_t = u_{xx} + cu_x + F(x, u), \quad x \in [0, L], \quad (1.1)$$

with

$$F(x, u) = \begin{cases} g_+(u) & \text{if } x \in [a, b] \\ g_-(u) & \text{if } x \in [0, a) \cup (b, L]. \end{cases} \quad (1.2)$$

Here,  $u(x, t)$  represents the population density of a species. The diffusion coefficient is normalized to 1, and  $c \geq 0$  denotes the advection coefficient. The population growth is governed by  $g_-(u)$  on the subintervals  $[0, a)$  and  $(b, L]$ , and by  $g_+(u)$  on the subinterval  $[a, b]$ . We assume  $g_+(u) \geq g_-(u)$ , so that the interval  $[a, b]$  can be interpreted as a protection zone within the habitat. Relevant ecological examples related to (1.1) include species movement in streams and rivers, coastlines with dominant longshore currents, lake water columns influenced by gravity, and shifting habitats such as oases moved by wind or favorable climate zones displaced by global warming. Reaction-advection-diffusion models have been widely applied in ecological and biological studies [1–7]. Lou and Lutscher proposed biologically meaningful boundary conditions for species in advective environments [6]. In this paper, we consider the following boundary conditions:

$$u_x = a_0 u \quad \text{for } x = 0, \quad u = 0 \quad \text{for } x = L, \quad (1.3)$$

and demonstrate how positive steady-state solutions can be established under these conditions. (1.3) indicates that at  $x = 0$  the flux is proportional to the population density and  $x = L$  corresponds to a hostile boundary point. The analysis presented below can also be adapted to other types of boundary conditions, including those considered in [6]. Further discussion is provided in Section 5.

Population declines across many species result from factors including climate change, habitat degradation, overharvesting, and biological invasions. To mitigate these pressures, protection zones such as natural reserves have been widely established and demonstrated to be effective in conserving habitats and biodiversity (e.g., [8–12]). Previous studies show that protection zones of sufficient size can enhance species persistence, whereas smaller zones may give rise to more complex dynamics that depend on species characteristics and habitat structure (see [1, 2, 4, 5, 7, 13] and references cited therein). Most existing partial differential equation models incorporating protection zones assume either no advection ( $c = 0$ ) or monostable growth dynamics, where the system has two steady states: an unstable extinction state and a stable carrying capacity. In contrast, a strong Allee effect characterized by bistability occurs when the per-capita growth rate increases at low population densities. A strong Allee effect, in particular, involves a critical threshold below which the population declines toward extinction [14, 15]. Many populations of conservation concern experience strong Allee effects and are managed within spatially protected areas. For instance, exploited populations such as Atlantic cod (*Gadus morhua*) can exhibit reduced growth at low densities and benefit from marine protected areas that provide spatial refuges and promote recovery [16], while in marine systems, protected areas can enhance persistence of populations subject to Allee-type thresholds [17]. In a recent study, Jin et al. [4] examined system (1.1) with growth function (1.2) under the assumption  $c = 0$ , where  $g_-$  exhibits a strong Allee effect and  $g_+$  is monostable. Using principal eigenvalue techniques, they established persistence results for several types of boundary conditions. In this paper, we investigate system (1.1) with (1.2) under the more general case  $c \geq 0$ , where both  $g_-$  and  $g_+$  exhibit strong Allee effects. One example illustrating the connection between  $g_+$  and  $g_-$  is  $g_-(u) = g_+(u) - \alpha u$  with  $\alpha > 0$ , representing the effect of species protection. In this context,  $\alpha$  models an additional harvesting rate in the unprotected region.

We assume that the integral of  $g_+(u)$  from 0 to its carrying capacity is positive, while that of  $g_-(u)$  is negative. The negativity of this integral implies that, for system (1.1) with  $c = 0$  and  $F(x, u) \equiv g_-(u)$  for  $-\infty < x < \infty$ , any compactly supported initial condition will lead to extinction. Our approach differs from that of Jin et al. [4] and is instead closely related to the work of Li and Otto [5] which

studied a reaction-diffusion equation with a strong Allee effect in a bounded habitat shifting at constant speed. When Allee effects are present throughout the habitat, studying eigenvalue problems for the corresponding linearized systems may not be sufficient to understand population dynamics; a global analysis of the full nonlinear system is required. The global phase plane analysis in a shifting bounded habitat with  $g_+ = g_-$ , presented in [5], provides a useful tool for studying (1.1)–(1.2). We show that the existence of positive steady-state solutions depends critically on the length of the protection zone. Specifically, there exists a threshold  $H^*$  such that (i) if the protection zone has length exactly  $H^*$ , a positive steady-state solution exists; (ii) if the zone is longer than  $H^*$ , multiple positive steady-state solutions exist; and (iii) if the zone is shorter than  $H^*$ , no positive steady-state solution exists. Finally, we support our analytical findings with numerical simulations illustrating the existence, stability, and structure of steady-state solutions.

This paper is organized as follows. Some preliminary results are given in Section 2. The main results regarding the existence of steady-state solutions are presented in Section 3. The numerical simulations are provided in Section 4. Some concluding remarks are discussed in Section 5.

## 2. Preliminary results

We begin with the following hypotheses:

**Hypotheses 2.1.** Let  $k_+ > 1$  be a constant.

- i.  $g_- \in C^1([0, \infty))$ ,  $g_-(0) = g_-(1) = 0$ ,  $g'_-(0) < 0$ , and  $g'_-(1) < 0$ . For some constant  $\alpha_- \in (0, 1)$ ,  $g_-(u) > 0$  for  $u \in (\alpha_-, 1)$ , and  $g_-(u) < 0$  for  $u \in (0, \alpha_-) \cup (1, k_+)$ .
- ii.  $g_+ \in C^1([0, \infty))$ ,  $g_+(0) = g_+(k_+) = 0$ , and  $g'_+(0) < 0$ ,  $g'_+(k_+) < 0$ . For some constant  $\alpha_+ \in (0, \alpha_-)$ ,  $g_+(u) > 0$  for  $u \in (\alpha_+, k_+)$ , and  $g_+(u) < 0$  for  $u \in (0, \alpha_+)$ .
- iii.  $g_+(u) \geq g_-(u)$  for  $u \in [0, k_+]$ , and  $g'_+(0) > g'_-(0)$ .
- iv.  $\int_0^1 g_-(u) du < 0$  and  $\int_0^{k_+} g_+(u) du > 0$ .

A prototype example of  $g_-(w)$  is  $g_-(w) = w(1-w)(w - \alpha_-)$  where  $0.5 < \alpha_- < 1$ , and an example of  $g_+(w)$  is  $g_+(w) = w(k_+ - w)(w - \alpha_+)$  where  $k_+ > 1$  and  $0 < \alpha_+ < 0.5$ . The integral conditions in Hypotheses 2.1 (iv) are satisfied by these two functions.

Under the condition  $\int_0^{k_+} g_+(u) du > 0$ , the reaction-diffusion equation

$$u_t = u_{xx} + g_+(u), \quad -\infty < x < \infty,$$

has a unique (up to translation) nonincreasing traveling wave with speed  $c_+^* > 0$ , and values 0 and  $k_+$  at  $\pm\infty$ , respectively. Similarly, with  $\int_0^1 g_-(u) du < 0$ , the equation

$$u_t = u_{xx} + g_-(u), \quad -\infty < x < \infty,$$

has a unique (up to translation) nonincreasing traveling wave with speed  $c_-^* < 0$ , and values 0 and 1 at  $\pm\infty$ , respectively [18]. A traveling wave with a positive speed moves forward, while one with a negative speed moves backward. With  $g_{\pm}(u) = w(k_{\pm} - w)(w - \alpha_{\pm})$  and  $k_- = 1$ , the speed can be explicitly given by

$$c_{\pm}^* = \frac{k_{\pm} - 2\alpha_{\pm}}{\sqrt{2}}.$$

See Hadeler and Rothe [3] and Nagumo et al. [19]. In general, the speed of a traveling wave with a bistable growth functions can be obtained using the variational formula given by Benguria and Depassier [20]. Specifically,

$$(c_+^*)^2 = \max_{h(u) \in C^1[0, k_+], h'(u) < 0} \left\{ \frac{2 \int_0^{k_+} g_+(u)h(u)du}{\int_0^{k_+} (-h^2(u)/h'(u))du} \right\},$$

and  $(c_-^*)^2$  is given by the right-hand side of this formula with  $k_+$  replaced by 1 and  $g_+(u)$  replaced by  $-g_-(1 - u)$ .

Consider the equations

$$u_t = u_{xx} + cu_x + g_{\pm}(u), \quad x \in (-\infty, \infty).$$

A steady-state solution  $u(x, t) = w(x)$  satisfies

$$w_{xx} + cw_x + g_{\pm}(w) = 0, \quad x \in (-\infty, \infty),$$

which are equivalent to the planar systems

$$\begin{aligned} w' &= v, \\ v' &= -cv - g_{\pm}(w). \end{aligned} \tag{2.1}$$

Phase plane analysis for (2.1) was conducted in Li and Otto [5] for the case of  $g_+$ . We shall further examine (2.1) as we need understand connections between the trajectories of the two systems. There are fixed points  $(0, 0)$ ,  $(\alpha_{\pm}, 0)$ , and  $(k_{\pm}, 0)$  where  $k_- = 1$  denotes the  $g_-(w)$  system carrying capacity for convenience of notation. For  $c > 0$ , the fixed points  $(0, 0)$  and  $(k_{\pm}, 0)$  are saddles. Let  $S_0^+$  and  $U_0^+$  denote, respectively, the stable and unstable manifolds of  $(0, 0)$  in the  $g_+(w)$  system for  $w \in (0, k_+)$ . Similarly let  $S_{k_+}^+$  and  $U_{k_+}^+$  denote the stable and unstable manifolds of  $(k_+, 0)$  for  $w \in (0, k_+)$ . Let  $S_0^-$ ,  $U_0^-$ ,  $S_1^-$ , and  $U_1^-$  denote the manifolds of the  $g_-(w)$  system, where the subscript denotes the corresponding fixed point and the superscript denotes the system.

The Jacobian matrix of system (2.1) is given by

$$J = \begin{pmatrix} 0 & 1 \\ -g'_{\pm}(w) & -c \end{pmatrix}.$$

The  $g_+(w)$  system has eigenvalues at  $(0, 0)$  of  $\lambda_0^{\pm} = \frac{-c \pm \sqrt{c^2 - 4g'_+(0)}}{2}$  and at  $(k_+, 0)$  of  $\lambda_{k_+}^{\pm} = \frac{-c \pm \sqrt{c^2 - 4g'_+(k_+)}}{2}$  with eigenvectors  $\begin{pmatrix} 1 \\ \lambda_0^{\pm} \end{pmatrix}$  and  $\begin{pmatrix} 1 \\ \lambda_{k_+}^{\pm} \end{pmatrix}$  respectively. Similarly, the  $g_-(w)$  system has eigenvalues at  $(0, 0)$  of  $\mu_0^{\pm} = \frac{-c \pm \sqrt{c^2 - 4g'_-(0)}}{2}$  and at  $(k_-, 0)$  of  $\mu_{k_-}^{\pm} = \frac{-c \pm \sqrt{c^2 - 4g'_-(k_-)}}{2}$  with eigenvectors  $\begin{pmatrix} 1 \\ \mu_0^{\pm} \end{pmatrix}$  and  $\begin{pmatrix} 1 \\ \mu_{k_-}^{\pm} \end{pmatrix}$  respectively. These together with Hypotheses 2.1 (iii) show that  $0 < \mu_0^+ < \lambda_0^+$ ,  $\lambda_0^- < \mu_0^- < 0$ . On the other hand, clearly  $\mu_{k_-}^-, \lambda_{k_+}^- < 0 < \mu_{k_-}^+, \lambda_{k_+}^+$ .

In consideration of the fact that a stable or unstable manifold at a fixed point is tangent to the line passing through the fixed point with its slope given by the corresponding eigenvector, the following lemma holds.

**Lemma 2.1.** Assume that Hypotheses 2.1 (i–iii) hold.

- i. Near  $(0, 0)$ ,  $S_0^+$  lies below the  $w$ -axis and  $U_0^+$  lies above the  $w$ -axis. Furthermore, near  $(0, 0)$ ,  $S_0^+$  is above  $S_0^-$  and  $U_0^+$  is below  $U_0^-$ .
- ii. Near  $(1, 0)$ ,  $S_1^-$  lies above the  $w$ -axis and  $U_1^-$  lies below the  $w$ -axis. Near  $(k_+, 0)$ ,  $S_{k_+}^+$  lies above the  $w$ -axis and  $U_{k_+}^+$  lies below the  $w$ -axis.

**Lemma 2.2.** Assume Hypotheses 2.1 hold.

- i.  $S_0^+$  is above  $S_0^-$  whenever  $v < 0$ . Furthermore,  $U_0^+$  is below  $U_0^-$  whenever  $v > 0$ .
- ii.  $U_1^-$  is above  $U_{k_+}^+$  whenever  $v < 0$ . Furthermore,  $S_1^-$  is below  $S_{k_+}^+$  whenever  $v > 0$ .

*Proof.* The proof of the statement (i) is similar to that of Lemma 4.14 in Fife [18] (also see Kanel' [21] and Li and Otto [5]) where different values of  $c$  and the same growth are considered. When  $v \neq 0$ ,  $v$  can be viewed as a function of  $w$ , and

$$\frac{dv}{dw} = -c - \frac{g(w)}{v}. \quad (2.2)$$

For the first part of statement (i), let  $v = v_-(w)$  represent  $S_0^-$  and  $v = v_+(w)$  represent  $S_0^+$  for  $v < 0$ . Our goal is to show these two curves do not intersect whenever  $v < 0$ . Define

$$S(w) =: v_+(w) - v_-(w).$$

Following this and (2.2), we obtain

$$\begin{aligned} \frac{dS}{dw} &= \frac{g_-(w)}{v_-(w)} - \frac{g_+(w)}{v_+(w)}, \\ \frac{dS}{dw} &= \frac{g_-(w)v_+(w) - g_+(w)v_-(w)}{v_+(w)v_-(w)}, \\ \frac{dS}{dw} &= \frac{g_-(w)v_+(w) - g_+(w)v_-(w) + g_-(w)v_-(w) - g_-(w)v_-(w)}{v_+(w)v_-(w)}, \\ \frac{dS}{dw} &= \frac{g_-(w)}{v_+(w)v_-(w)}S + \frac{v_-(w)(g_-(w) - g_+(w))}{v_+(w)v_-(w)}. \end{aligned}$$

We treat this equation as linear in  $S$  and derive an explicit expression for  $S$ . Let  $w_0$  be a small value of  $w$  guaranteed by the eigenvectors such that  $v_+(w) - v_-(w) > 0$  whenever  $0 < w \leq w_0$ . Applying the standard integrating factor method yields

$$\begin{aligned} \frac{dS}{dw} e^{\int_{w_0}^w -\frac{g_-(y)}{v_+(y)v_-(y)} dy} - \frac{g_-(w)}{v_+(w)v_-(w)} S e^{\int_{w_0}^w -\frac{g_-(y)}{v_+(y)v_-(y)} dy} \\ = \frac{v_-(w)(g_-(w) - g_+(w))}{v_+(w)v_-(w)} e^{\int_{w_0}^w -\frac{g_-(y)}{v_+(y)v_-(y)} dy}, \end{aligned}$$

$$\frac{d}{dw} (S e^{\int_{w_0}^w -\frac{g_-(y)}{v_+(y)v_-(y)} dy}) = \frac{v_-(w)(g_-(w) - g_+(w))}{v_+(w)v_-(w)} e^{\int_{w_0}^w -\frac{g_-(y)}{v_+(y)v_-(y)} dy},$$

$$S e^{\int_{w_0}^w -\frac{g_-(y)}{v_+(y)v_-(y)} dy} = \int_{w_0}^w \frac{v_-(w)(g_-(w) - g_+(w))}{v_+(w)v_-(w)} e^{\int_{w_0}^w -\frac{g_-(y)}{v_+(y)v_-(y)} dy} dw.$$

By Lemma 2.1, it is known that, for  $w \in (0, w_0]$ ,  $S_0^+$  is above  $S_0^-$  below the  $w$ -axis. Assume by way of contradiction that  $S_0^+$  crosses  $S_0^-$  for some value  $1 \geq w > w_0$ , namely that  $S(w) = v_+(w) - v_-(w) = 0$ . Then,

$$\int_{w_0}^w \frac{v_-(w)(g_-(w) - g_+(w))}{v_+(w)v_-(w)} e^{\int_{w_0}^w -\frac{g_-(y)}{v_+(y)v_-(y)} dy} dw = 0.$$

But, the integrand is necessarily positive whenever  $v_+(w)$  and  $v_-(w)$  are below the  $w$ -axis. Thus,  $S_0^+$  is above  $S_0^-$  whenever  $v < 0$ .

For the second part of statement (i) regarding the stable manifolds of 0 above the  $w$ -axis, let  $v = v_-(w)$  represent  $U_0^-$  and  $v = v_+(w)$  represent  $U_0^+$  for  $v > 0$ . In this case,  $v_-(w) - v_+(w) > 0$  for  $w$  near 0. Let  $w_0$  be a value of  $w$  such that  $v_-(w) - v_+(w) > 0$  for  $w \in (0, w_0]$ . Defining

$$T =: v_-^+ - v_+^+,$$

similar manipulations with an integrating factor of

$$e^{\int_{w_0}^w -\frac{g_+(y)}{v_+(y)v_+^+(y)} dy}$$

yield

$$\frac{d}{dw} T e^{\int_{w_0}^w -\frac{g_+(y)}{v_+(y)v_+^+(y)} dy} = \frac{v_+^+(w)(g_+(w) - g_-(w))}{v_+(w)v_+^+(w)} e^{\int_{w_0}^w -\frac{g_+(y)}{v_+(y)v_+^+(y)} dy},$$

$$\int_{w_0}^w \frac{d}{dw} T e^{\int_{w_0}^w -\frac{g_+(y)}{v_+(y)v_+^+(y)} dy} dw = \int_{w_0}^w \frac{v_+^+(w)(g_+(w) - g_-(w))}{v_+(w)v_+^+(w)} e^{\int_{w_0}^w -\frac{g_+(y)}{v_+(y)v_+^+(y)} dy} dw,$$

$$T e^{\int_{w_0}^w -\frac{g_+(y)}{v_+(y)v_+^+(y)} dy} = \int_{w_0}^w \frac{v_+^+(w)(g_+(w) - g_-(w))}{v_+(w)v_+^+(w)} e^{\int_{w_0}^w -\frac{g_+(y)}{v_+(y)v_+^+(y)} dy} dw.$$

The integrand on the right-hand side is positive whenever  $v_-^+$  and  $v_+^+$  are above the  $w$ -axis, so the assumption that  $T = 0$  for any corresponding value of  $w$  would yield a contradiction.

For the first part of statement (ii), let  $v = v_-(w)$  represent  $U_1^-$  and  $v = v_+(w)$  represent  $U_{k_+}^+$  for  $v < 0$ . Since  $k_+ > 1$ , there exists some  $w_1$  close to 1 such that  $U_1^-$  is above  $U_{k_+}^+$  whenever  $w \in [w_1, 1]$ . Define

$$T(w) =: v_-^- - v_+^-.$$

Similar manipulations yield

$$T e^{\int_{w_1}^w -\frac{g_+(y)}{v_+(y)v_+^-(y)} dy} = \int_{w_1}^w \frac{v_+^-(w)(g_+(w) - g_-(w))}{v_+(w)v_+^-(w)} e^{\int_{w_1}^w -\frac{g_+(y)}{v_+(y)v_+^-(y)} dy} dw.$$

Here, the integrand on the right-hand side is nonzero whenever  $v_-^-$  and  $v_+^-$  are below the  $w$ -axis, so the assumption that  $T = 0$  for any relevant value of  $w$  would yield a contradiction. This proves the first part of statement (ii). The proof of the second part of statement (ii) is similar and omitted. This concludes the proof.

The previous lemmas have not been dependent on the sign of the  $\int_0^{k_{\pm}} g_{\pm}(w) dw$ . Phase plane analysis for the system was done by Li and Otto [5] when  $\int_0^{k_+} g_+(w) dw > 0$  with varying  $c$  and by Johnson [22] for the system when  $\int_0^{k_-} g_-(w) dw < 0$  with  $c = 0$ . To study the systems as  $c$  varies, we use  $S_{0,c}^{\pm}$ ,  $S_{k_{\pm},c}^{\pm}$ ,  $U_{0,c}^{\pm}$ , and  $U_{k_{\pm},c}^{\pm}$  to denote stable and unstable manifolds at  $(0, 0)$  and  $(k_{\pm}, 0)$ , respectively. Here  $k_- = 1$  and the first subscript indicates the fixed point of the manifold and the second subscript indicates the value of  $c$ . As before, the superscript indicates that it is the  $g_+$  or  $g_-$  system under consideration. For simplicity, we shall continue to use  $S_0^{\pm}$ ,  $S_{k_{\pm}}^{\pm}$ ,  $U_0^{\pm}$ , and  $U_{k_{\pm}}^{\pm}$  to denote the stable and unstable manifolds when there is no ambiguity regarding  $c$ .

As argued in Li and Otto [5], Eq (2.1) yields origin manifolds of

$$S_{0,c}^- \text{ and } U_{0,c}^- : \frac{1}{2}v^2 = \int_0^w g_-(s) ds$$

and  $(1, 0)$  manifolds of

$$S_{1,0}^- \text{ and } U_{1,0}^- : v = \pm \sqrt{2 \int_w^1 g_-(s) ds}.$$

For a visual representation of the following lemma, see Figure 1. For more information, see [5, 22]. Li and Otto [5] provided phase plane analysis for the case that the growth function is  $g_+$  in a bounded habitat with proper boundary conditions. The analysis is related to the nonincreasing traveling wave of the corresponding system in the unbounded habitat  $(-\infty, \infty)$ . We use  $T^*$  to denote the trajectory corresponding to the nonincreasing traveling wave with speed  $c_+^* > 0$  in the phase plan. It is a heteroclinic orbit in the fourth quadrant connecting  $(0, 0)$  to  $(k_+, 0)$ . The following lemma follows from Lemma 2.4 in [5].

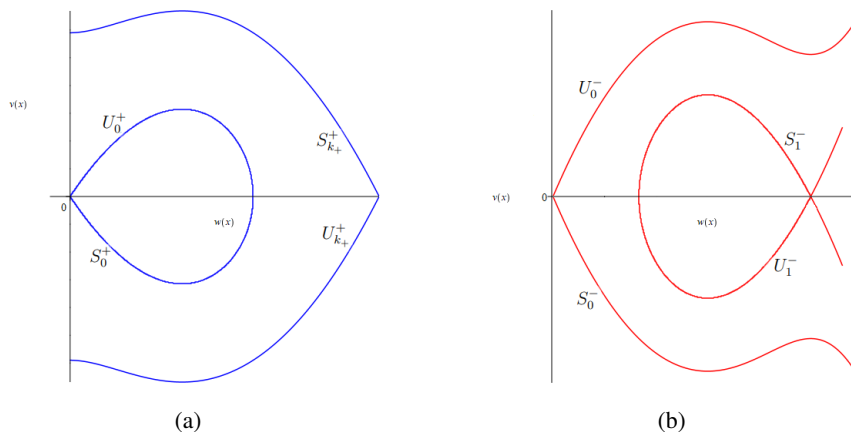


**Figure 1.** (a) Stable and unstable manifolds of a generic  $g_+(w)$  system with carrying capacity  $k_+$  in which  $\int_0^{k_+} g_+(w) dw > 0$  and  $c = 0$ . (b) Stable and unstable manifolds of a generic  $g_-(w)$  system with carrying capacity  $k_-$  in which  $\int_0^{k_-} g_-(w) dw < 0$  and  $c = 0$ .

**Lemma 2.3.** Assume that Hypotheses 2.1 hold and  $c_+^* > c > 0$ . We have the following statements:

- i.  $S_{k_+,c}^+$  lies above  $S_{k_+,0}^+$ , and below a line  $v = -m(w - k_+)$  with  $m > 0$ .

- ii.  $U_{k_+,c}^+$  lies above  $U_{k_+,0}^+$  and below  $T^*$ , and  $U_{k_+,c}^+$  and  $S_{0,c}^+$  do not intersect.
- iii.  $S_{0,c}^+$  lies outside the loop  $S_{0,0}^+$  and  $U_{0,0}^+$ , below  $S_{k_+,c}^+$ , and above  $U_{k_+,c}^+$ .
- iv.  $U_{0,c}^+$  lies inside the loop  $S_{0,0}^+$  and  $U_{0,0}^+$  and approaches  $(\alpha_+, 0)$ .

A graphical demonstration for  $S_0^\pm$ ,  $U_0^+$ ,  $S_{k_+}^+$ , and  $U_{k_+}^+$  is given in Figure 2.

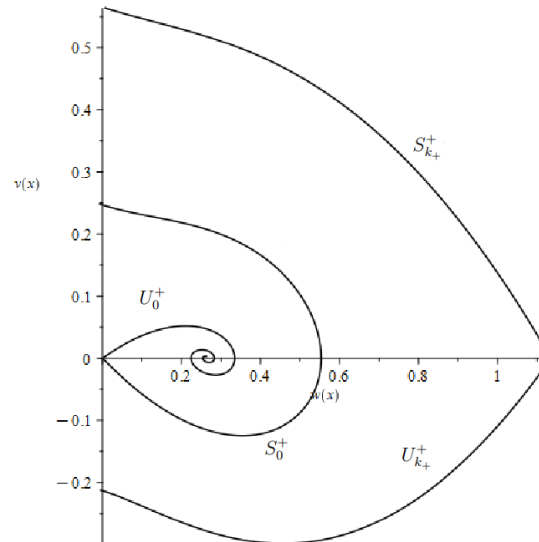


**Figure 2.** Stable and unstable manifolds of  $(0, 0)$  and  $(k_+, 0)$  for a generic  $g_+(w)$  system with  $\int_0^{k_+} g_+(w) dw > 0$  and  $c_+^* > c > 0$ . The specific system is given with  $g_+(w) = w(1 - w)(w - 0.4) + 0.1w$  and  $c = 0.1$ .

**Lemma 2.4.** Assume  $c > 0$ .

- i.  $U_{0,c}^-$  lies below  $U_{0,0}^-$ , and  $S_{0,c}^-$  lies below  $S_{0,0}^-$ .
- ii.  $U_{1,c}^-$  remains inside the homoclinic loop  $S_{1,0}^-$  and  $U_{1,0}^-$ , and  $S_{1,c}^-$  approaches the point  $(\alpha_-, 0)$ .
- iii.  $S_{1,c}^-$  remains outside of the homoclinic loop  $S_{1,0}^-$  and  $U_{1,0}^-$ .

*Proof.* Statement (i) follows from Lemmas 2.2 and 2.3 of Li and Otto [5]. Lemma 2.2 states that for  $c_2 > c_1 \geq 0$  the manifolds of  $(0, 0)$  for the  $c_2$  system lie below those of the  $c_1$  system near the origin, and that the manifolds of  $(1, 0)$  for the  $c_2$  system lie above those of the  $c_1$  system near  $(1, 0)$ . Further, the proof of Lemma 2.2 gives that if two trajectories from two systems corresponding to different  $c$  values do not intersect at some value  $w$ , they must remain apart on that side of the  $w$ -axis. This leads to statement (i).

For statement (ii), suppose  $c > 0$ . Since  $U_{1,c}^-$  is above  $U_{1,0}^-$  of  $(1, 0)$ , it must remain above  $U_{1,0}^-$  when  $v < 0$  and must intersect the  $w$ -axis at some point  $(w_c, 0)$  such that  $w_c$  is greater than the value of  $w$  at which  $U_{1,0}^-$  intersects the  $w$ -axis. This implies that  $U_{1,0}^-$  is above  $U_{1,c}^-$  at  $w_c$  for  $v > 0$ , and so remains above  $U_{1,c}^-$  when  $v > 0$ . Thus,  $U_{1,c}^-$  remains inside the homoclinic loop formed by  $S_{1,0}^-$  and  $U_{1,0}^-$ , and by the Poincaré-Bendixson theorem approaches the fixed point  $(\alpha_-, 0)$ .

Since  $S_{1,c}^-$  is above  $S_{1,0}^-$ ,  $S_{1,c}^-$  remains above  $S_{1,0}^-$  when  $v > 0$  by prior arguments. Likewise, when  $v < 0$ ,  $S_{1,c}^-$  is below  $S_{1,0}^-$  at the value of  $w$  at which  $S_{1,0}^-$  intersects the  $w$ -axis. Thus,  $S_{1,c}^-$  remains below

$S_{1,0}^-$ . Therefore,  $S_{1,c}^-$  remains outside of the homoclinic loop formed by  $U_{1,0}^-$  and  $S_{1,0}^-$ . This completes the proof.

A graphical demonstration for  $S_0^-$ ,  $U_0^-$ ,  $S_{k_+}^-$ , and  $U_{k_+}^-$  is given in Figure 3.

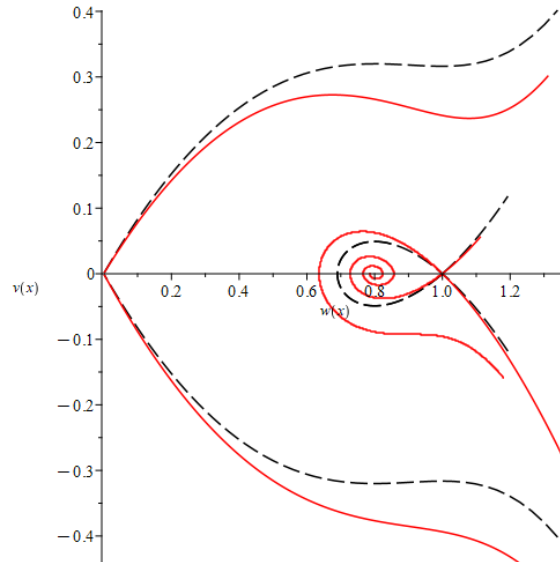


**Figure 3.** Stable and unstable manifolds (red) of  $(0, 0)$  and  $(1, 0)$  for a generic  $g_-(w)$  system with  $\int_0^{k_+} g_-(w) dw < 0$ . The specific system is given with  $g_-(w) = w(1 - w)(w - 0.8)$ , having  $\int_0^{k_+} g_+(w) dw = -0.05$  and  $c = 0.1$ . (red). The previous system with  $c = 0$  is superimposed (dotted black).

It is necessary to establish how the trajectories of the  $g_+(w)$  and  $g_-(w)$  systems interact when the systems are considered in the same plane. Particularly, it is important to study how trajectories from the systems behave at their intersections.

- Lemma 2.5.** *i. Suppose that a trajectory in the  $g_+(w)$  system intersects a trajectory in the  $g_-(w)$  system for some  $w = w^*$ . Then, the two trajectories must cross the  $w -$  axis before they can intersect again.*
- ii. Suppose two trajectories  $v_+^+(w)$  and  $v_-^+(w)$ , corresponding to  $g_+(w)$  and  $g_-(w)$  respectively, intersect above the  $w$ -axis at  $w = w^*$ . Then, for  $w > w^*$ ,  $v_+^+(w) > v_-^+(w)$  above the  $w$ -axis. If two trajectories  $v_+^-(w)$  and  $v_-^-(w)$  intersect below the  $w$ -axis at  $w = w^-$ , then for  $w < w^-$ ,  $v_-^-(w) > v_+^-(w)$  below the  $w$ -axis.*

*Proof.* For part (i), let  $v = v_-(w)$  and  $v = v_+(w)$  represent trajectories in the  $g_+(w)$  and  $g_-(w)$  systems such that  $v_-(w^*) = v_+(w^*)$  for  $w^* \in [0, 1]$  and that  $v_-(w) > v_+(w)$  for  $w$  near  $w^*$  but slightly greater. Then, in light of Eq (2.1), prior calculations from Lemma 1 using  $T(w) =: v_-(w) - v_+(w)$  and an integrating factor of  $e^{\int_{w^*}^w -\frac{g_+(y)}{v_+(y)v_-(y)} dy}$  yield

$$T e^{\int_{w^*}^w -\frac{g_+(y)}{v_+(y)v_-(y)} dy} = \int_{w^*}^w \frac{v_+(w)(g_+(w) - g_-(w))}{v_+(w)v_-(w)} e^{\int_{w^*}^w -\frac{g_+(y)}{v_+(y)v_-(y)} dy} dw,$$

whose right-hand side has a strictly positive integrand as long as  $v_-(w), v_+(w)$  are above the  $w$ -axis and a strictly negative integrand whenever  $v_+(w), v_-(w)$  are below the  $w$ -axis. Thus, for  $w > w^*$ ,  $T$  cannot be zero, and the two trajectories cannot intersect without crossing the  $w$ -axis.

Likewise, suppose that  $S(w) =: v_+(w) - v_-(w) > 0$  for  $w$  near  $w^*$  but slightly less. Using an integrating factor of  $e^{\int_{w^*}^w -\frac{g_-(y)}{v_+(y)v_-(y)} dy}$  and similar calculations, the equation

$$S e^{\int_{w^*}^w -\frac{g_-(y)}{v_+(y)v_-(y)} dy} = \int_{w^*}^w \frac{v_-(w)(g_-(w) - g_+(w))}{v_+(w)v_-(w)} e^{\int_{w^*}^w -\frac{g_-(y)}{v_+(y)v_-(y)} dy} dw$$

has a right-hand side integrand which is strictly positive whenever  $v_+(w), v_-(w)$  are above the  $w$ -axis and strictly negative whenever  $v_+(w), v_-(w)$  are below the  $w$ -axis. Part (ii) shows that these are the only cases that need to be proven. Thus, for  $w < w^*$ ,  $S$ , the two trajectories cannot intersect without crossing the  $w$ -axis.

For part (ii), let  $v_-^+(w)$  and  $v_+^+(w)$  be two trajectories of the  $g_-(w)$  and  $g_+(w)$  systems respectively, which are above the  $w$ -axis. Suppose  $v_-^+(w^*) = v_+^+(w^*)$ . Equation (2.1) and Hypothesis 2.1 (iii) yields

$$\begin{aligned} g_-(w^*) &< g_+(w^*), \\ -c - \frac{g_-(w^*)}{v_-^+(w^*)} &> -c - \frac{g_+(w^*)}{v_+^+(w^*)}, \\ \frac{dv_-^+}{dw} \Big|_{w^*} &> \frac{dv_+^+}{dw} \Big|_{w^*}. \end{aligned}$$

Therefore, if the two trajectories intersect above the  $w$ -axis, the  $g_-(w)$  system trajectory stays above the  $g_+(w)$  system trajectory for some interval of  $w$  to the right of the intersection point. Statement (i) of this lemma gives that this separation remains true as long as the trajectories are above the  $w$ -axis. For the case below the  $w$ -axis, similar calculations on trajectories  $v_-^-(w)$  and  $v_+^-(w)$  which intersect at  $w = w^*$  yield

$$\frac{dv_-^-}{dw} \Big|_{w^*} > \frac{dv_+^-}{dw} \Big|_{w^*}.$$

Thus, by similar arguments, if the two trajectories intersect below the  $w$ -axis, the  $g_-(w)$  trajectory stays above the  $g_+(w)$  trajectory for  $w$  values to the left of the intersection point.

### 3. Main results

Let  $I$  denote the segment of the line  $v - a_0w = 0$  from  $(0, 0)$  to its intersection with  $S_{k_+}^+$ , where  $a_0$  is a positive constant. Let  $A$  be the region bounded by the  $v$ -axis,  $S_{k_+}^+$ , the  $w$ -axis, and  $S_0^+$ . Let  $B$  denote the  $v$ -axis inside  $U_{k_+}^+$  along with the open region bounded by the  $v$ -axis,  $U_{k_+}^+$  and bounded above by  $S_0^-$ . See Figure 4. Let  $T_p$  be a trajectory from the line  $v - a_0w = 0$  to the line  $w = 0$  below the  $w$ -axis with  $T_p|_{x=0} =: (w_0, v_0)$  and  $T_p|_{x=L} = q = (0, v_L)$ . In general, let  $(w_{x^*}, v_{x^*})$  denote  $T_p|_{x=x^*}$  for any  $x^* \in [0, L]$ . Suppose for  $a, b, L \in \mathbb{R}$  with  $0 \leq a \leq b \leq L$  that  $T_p$  acts according to the  $g_-(w)$  system for  $x \in [0, a]$ , according to the  $g_+(w)$  system for  $x \in [a, b]$ , and once again according to the  $g_-(w)$  system for  $(b, L]$ . The equation

$$v = \frac{dw}{dx}$$

yields that for any position  $x$  and corresponding point  $(w_x, v_x)$ ,

$$\int_{w_0}^{w_x} \frac{1}{v} dw = x.$$

Thus

$$a = \int_{w_0}^{w_a} \frac{1}{v^+} dw \text{ and } b = \int_{w_b}^0 \frac{1}{v^-} dw.$$

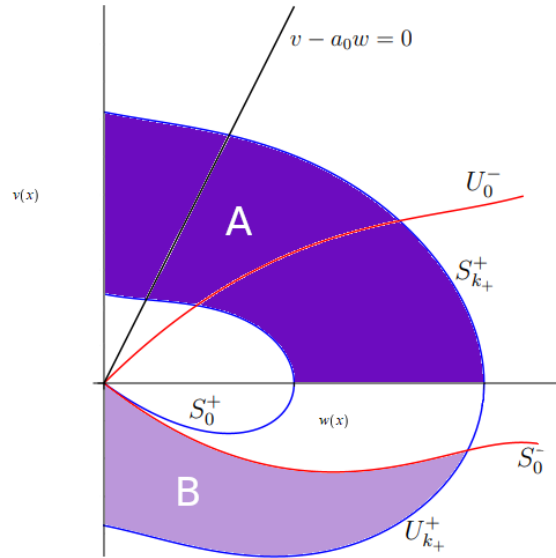


**Figure 4.** Relevant stable and unstable manifolds for the  $g_+(w)$  system (blue) and the  $g_-(w)$  system (red), along with important regions of viability for a trajectory which acts according to the  $g_-(w)$  system for  $x \in [0, a) \cup (b, L]$  and according to the  $g_+(w)$  system for  $x \in [a, b]$ . Trajectories evaluated at  $x = a$  must be inside the region A (dark purple) and evaluated at  $x = b$  must be inside the region B (light purple). Trajectories evaluated at  $x = 0$  are on the line  $v - a_0w = 0$  inside  $S_{k_+}^+$  and evaluated at  $x = L$  are on the negative  $v$ -axis. Note that the relation of the line  $v - a_0w = 0$  to  $U_0^-$  determines which subregion of A is relevant for a given system.

Suppose for fixed  $p$  that  $T_p$  intersects  $S_{k_+}^+$  at  $(w_{a^*}, v_{a^*})$ . Any trajectory that intersects  $S_{k_+}^+$  must achieve or go beyond the carrying capacity  $k_+$ , since by Lemma 3.1  $T_p$  cannot re-enter A once it has left. Any such trajectory is biologically irrelevant and so is discarded. Further, trajectories in the  $g_-(w)$  system cannot reach the  $w$ -axis in a finite distance  $x$ . Finally, trajectories above the  $w$ -axis are increasing in  $w$  as  $x$  increases since  $\frac{dw}{dx} = v > 0$ . From these statements, we conclude that  $T_p|_{x=a}$  must be inside the region A and

$$a < \int_{w_0}^{w_{a^*}} \frac{1}{v^+} dw.$$

Since trajectories in the  $g_-(w)$  system are unique, any trajectory that intersects the  $v$ -axis with  $v < 0$  must remain below  $U_0^-$  for  $x \in (b, L]$ . Further,  $T_p|_{x=b}$  cannot be below  $U_{k_+}^+$  since that would imply

that  $w(x)$  was beyond the carrying capacity  $k_+$  for some  $x \in (a, b)$ . Therefore,  $T_p|_{x=b} \in B$  and

$$L - b < \int_{w_{b^*}}^0 \frac{1}{v^-} dw.$$

Fix  $a > 0$  and let  $f_a : I \rightarrow \mathbb{R} \times \mathbb{R}$  map the initial point  $p$  to the point  $T_p|_a$ . Then,  $f_a$  is continuous (see Theorem 1.3.1 in [23]) and for  $a_2 > a_1$ ,  $w_{a_2} > w_{a_1}$  since  $\frac{dw}{dx} = v > 0$ . See a graphical demonstration of  $f_a$  in Figure 5(a).

**Lemma 3.1.** *Let  $D_a$  denote the set of points  $p = (w_0, v_0)$  for fixed  $a$  such that  $T_p|_a \in A$ . For  $a_2 > a_1$ ,  $D_{a_2} \subseteq D_{a_1}$ .*

*Proof.* Suppose  $p = (w_0, v_0) \in D_{a_2}$ . Then,  $w_{a,p} < w_{a^*,p}$  where  $w_{a,p}$  is the  $w$  value of  $T_p|_a$  and  $w_{a^*,p}$  is the value of  $w$  at which a trajectory in the  $g_-(w)$  system starting at  $p$  intersects  $S_{k_+}^+$ . Since  $a_2 > a_1 \implies w_{a_2,p} > w_{a_1,p}$ ,  $w_{a_1,p} \leq w_{a_2,p} < w_{a^*,p}$ . Since a trajectory in the  $g_-(w)$  system that starts above  $S_{k_+}^+$  cannot cross below  $S_{k_+}^+$  to be inside  $A$  by Lemma 2.5, and  $T_p \in A$  at  $w = w_{a_2,p}$ ,  $T_p \in A$  at  $w = w_{a_1,p}$  and so  $(w_0, v_0) \in D_{a_1}$ .

Let  $J$  denote the negative  $v$ -axis inside  $U_{k_+}^+$ . Fix  $L - b > 0$  and let  $f_b : J \rightarrow \mathbb{R} \times \mathbb{R}$  map points on  $J$  to the point reached by a trajectory in the  $g_-(w)$  system after traveling a distance of  $-(L - b)$  from  $J$ . Then,  $f_b$  is continuous [23]. See a graphical demonstration of  $f_b$  in Figure 5(b).

Recall that  $D_a$  denotes the set of points  $p$  on the line  $v - a_0w = 0$  such that  $T_p \in A$  at  $w = a$ , and let  $D_b$  denote the set of points  $p$  on the negative  $v$ -axis such that a trajectory from  $p$  traveling a distance of  $-(L - b)$  remains in  $B$ . By prior arguments, for  $b_1, b_2$  such that  $L - b_1 < L - b_2$ ,  $D_{b_2} \subseteq D_{b_1}$ . Fix  $a, b$  and consider the curves  $S_a = \{f_a(p)|p \in D_a\}$  and  $S_b = \{f_b(p)|p \in D_b\}$ . For any trajectory  $T_p$  with fixed  $a$  and  $L - b$ , let  $T_p^*$  denote the segment of the trajectory from  $S_a$  to  $S_b$ . Let  $p_a$  denote  $T_p|_{w=a}$ . The length of  $T_p^*$ ,  $b - a$ , is given as a function of  $p_a$  by

$$b - a = H(p_a) =: \int_{w_a}^{w^*} \frac{1}{v_+^+(p_a; w)} dw + \int_{w^*}^{w_b} \frac{1}{v_+^-(p_a; w)} dw, \tag{3.1}$$

where  $w^*$  is the intersection point of  $T_p$  and the  $w$ -axis, and  $v_+^+$  and  $v_+^-$  correspond to the  $g_+(w)$  system above and below the  $w$ -axis.

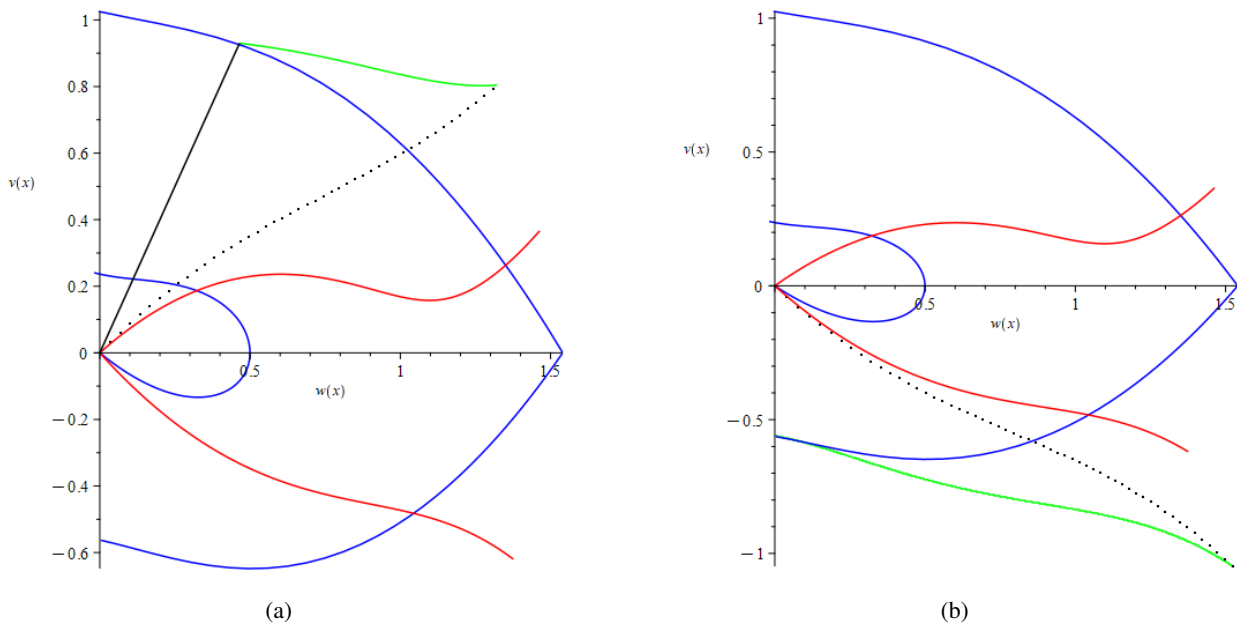


**Figure 5.** (a) Example  $f_a$  curve (dotted black). Points are generated by evaluating trajectories that begin on the line  $v = 2w$  at  $x = 1$ . Also included are essential  $g_+(w)$  system manifolds (blue) and  $g_-(w)$  system manifolds (red), along with an example trajectory (green) beginning at the maximum point on  $I$  from  $x = 0$  to  $x = 1$  (green). The specific system is given with  $g_-(w) = w(1 - w)(w - 0.8)$ ,  $r = 0.4$ , and  $c = 0.1$ . (b) Example  $f_b$  curve (dotted black). Also included are the manifolds from (a) along with an example trajectory (green) beginning at the minimum  $v$ -axis value inside  $U_{k_+}^+$

**Lemma 3.2.**  $H(p_a)$  is continuous in  $p_a$  for  $p_a \in S_a$

*Proof.* By prior arguments,  $f_a(p)$  is continuous with respect to  $p$ . Thus, for fixed  $a$ , the curve  $S_a$  is well defined with respect to  $p_a$  so that any  $p_a \in S_a$  corresponds to a unique trajectory  $T_p^*$ . Since  $g_+(w) \in C^1[0, 1]$ , the solution  $(w(x), v(x))$  along  $T_p^*$  depends on the initial values  $P_a$  (see Theorem 1.3.1 in [23]). Consequently,  $w_b$  and  $v_b$  depend continuously on  $p_a$ . Further,  $\frac{dw}{dx} = v$  is monotonic on each side of the  $w$ -axis so that  $x$  is a continuous function of  $w$ . Thus,  $v_+(p_a; w)$  is a continuous function of  $w$  for  $w \in [w_a, w^*]$ , and similarly  $v_-(p_a; w)$  is continuous for  $w \in [w_b, w^*]$ . Near  $(w^*, 0)$ ,  $\frac{dv}{dx} \approx -g_+(w^*) < 0$ , so that  $w$  is a function of  $v$  on  $T_p^*$ . Similar to arguments made in Lemma 2.5 of [5], it follows that

$$\left. \frac{dw(v)}{dv} \right|_{v=0} = - \left. \frac{v}{cv + g(w)} \right|_{w=w^*, v=0} = - \frac{0}{g(w^*)} = 0$$

and

$$\left. \frac{d^2w(v)}{dv^2} \right|_{v=0} = - \left. \frac{cv + g(w) - v(c + g'(w)\frac{dw}{dv})}{[cv + g(w)]^2} \right|_{w=w^*, v=0} = - \frac{1}{g(w^*)} < 0.$$

Thus, for any small  $\epsilon > 0$ , there exists  $\gamma > 0$  such that for  $w \in [w^* - \gamma, w^*]$ ,  $w > w^* + (-\frac{1}{g(w^*)} - \epsilon)v^2$ , so that

$$\frac{1}{|v|} < \sqrt{\left(\frac{1}{g(w^*)} + \epsilon\right) \frac{1}{w^* - w}}, \tag{3.2}$$

which is then true in particular for  $v_+^+(p_a; w)$ . Therefore,  $H(p_a)$  is well-defined.

Fix  $p_a \in S_a$  with  $p_a = (w_a, v_a)$ . Consider a trajectory  $T_{\tilde{p}}$  with  $T_{\tilde{p}}|_{x=a} = \tilde{p}_a = (\tilde{w}_a, \tilde{v}_a)$ , and  $\tilde{w}^*$  as the  $w$  value of its intersection with the  $w$ -axis. Assume  $\tilde{w}_a < w_a$  and that  $\tilde{p}_a \in S_a$ . By uniqueness,  $T_{\tilde{p}}$  is below  $T_p$  for  $v > 0$ . For any small  $\epsilon > 0$ , continuity and inequality (3.2) imply that there exists  $\delta_1 > 0$  such that for  $w_a - \tilde{w}_a < \delta_1$ ,

$$\int_{\tilde{w}^*}^{w_a} \frac{1}{v_+^+(p_a; w)} dw < \frac{\epsilon}{3}. \tag{3.3}$$

Let  $\tilde{v}_+^+(\tilde{p}_a; w)$  and  $\tilde{v}_-^+(\tilde{p}_a; w)$  denote  $T_{\tilde{p}}$  above and below the  $w$ -axis respectively. Choose  $w_s \in (w_a, \tilde{w}^*)$  with  $w_s$  sufficiently close to  $\tilde{w}^*$  such that

$$\int_{w_s}^{\tilde{w}^*} \frac{1}{\tilde{v}_+^+(\tilde{p}_a; w)} dw < \frac{\epsilon}{3}. \tag{3.4}$$

For  $\delta_2 = \tilde{v}_+^+(\tilde{p}_a; w_s) \frac{\epsilon}{3}$  and  $w_a - \tilde{w}_a < \delta_2$ ,

$$\int_{\tilde{w}_a}^{w_a} \frac{1}{\tilde{v}_+^+(\tilde{p}_a; w)} dw \leq \frac{w_a - \tilde{w}_a}{\tilde{v}_+^+(\tilde{p}_a; w_s)} < \frac{\epsilon}{3}. \tag{3.5}$$

Let  $S = v_+^+(p_a; w) - \tilde{v}_+^+(\tilde{p}_a; w)$  for  $w \in [w_a, w_s]$ . Equation (2.1) gives that

$$S' = -\frac{g(w)}{v_+^+(p_a; w)\tilde{v}_+^+(\tilde{p}_a; w)}S.$$

From this and since  $\tilde{v}_+^+(\tilde{p}_a; w) < v_+^+(p_a; w)$  for  $v > 0$ , it follows for  $w \in [p_a, w_s]$  that

$$\begin{aligned} S(w) &= S(w_a)e^{-\int_{w_a}^w \frac{g(y)}{v_+^+(p_a; y)\tilde{v}_+^+(\tilde{p}_a; y)} dy} \leq S(w_a)e^{-(w-w_a)\frac{g_{min}}{(\tilde{v}_+^+(\tilde{p}_a; w_s))^2}} \\ &\leq (v_+^+(p_a; p_a) - \tilde{v}_+^+(\tilde{p}_a; p_a))e^{-\frac{g_{min}}{(\tilde{v}_+^+(\tilde{p}_a; w_s))^2}}, \end{aligned}$$

where  $g_{min} < 0$  is the minimal value of  $g(w)$  for  $w \in [0, 1]$ . Thus,

$$\begin{aligned} \int_{w_a}^{w_s} \left( \frac{1}{\tilde{v}_+^+(\tilde{p}_a; w)} - \frac{1}{v_+^+(p_a; w)} \right) dw &= \int_{w_a}^{w_s} \frac{v_+^+(p_a; w) - \tilde{v}_+^+(\tilde{p}_a; w)}{v_+^+(p_a; w)\tilde{v}_+^+(\tilde{p}_a; w)} dw \\ &\leq (w_s - w_a) \frac{v_+^+(p_a; w_a) - \tilde{v}_+^+(\tilde{p}_a; w_a)}{(\tilde{v}_+^+(\tilde{p}_a; w_s))^2} e^{-\frac{g_{min}}{(\tilde{v}_+^+(\tilde{p}_a; w_s))^2}} \\ &\leq \frac{v_+^+(p_a; w_a) - \tilde{v}_+^+(\tilde{p}_a; w_a)}{(\tilde{v}_+^+(\tilde{p}_a; w_s))^2} e^{-\frac{g_{min}}{(\tilde{v}_+^+(\tilde{p}_a; w_s))^2}}. \end{aligned}$$

Since  $v_+^+(p_a; w_a) - \tilde{v}_+^+(\tilde{p}_a; w_a)$  approaches 0 as  $p_a$  approaches  $\tilde{p}_a$ , there exists  $\delta_3 > 0$  such that for  $w_a - \tilde{w}_a < \delta_3$ ,

$$\int_{w_a}^{w_s} \left( \frac{1}{\tilde{v}_+^+(\tilde{p}_a; w)} - \frac{1}{v_+^+(p_a; w)} \right) dw < \frac{\epsilon}{3}. \tag{3.6}$$

Let  $\delta = \min\{\delta_1, \delta_2, \delta_3\}$ . Then combining (3.3)–(3.6), we have that for  $w_a - \tilde{w}_a < \delta$ ,

$$\left| \int_{w_a}^{w_s} \left( \frac{1}{v_+^+(p_a; w)} \right) dw - \int_{\tilde{w}_a}^{\tilde{w}^*} \left( \frac{1}{\tilde{v}_+^+(\tilde{p}_a; w)} \right) dw \right| < \epsilon.$$

Similarly, for the given  $\epsilon$ , there exists  $\tilde{\delta}$  such that for  $w_a - \tilde{w}_a < \tilde{\delta}$ ,

$$\left| \int_{w_b}^{w_*} \left( \frac{1}{v_+^-(p_a; w)} \right) dw - \int_{\tilde{w}_b}^{\tilde{w}_*} \left( \frac{1}{\tilde{v}_+^-(\tilde{p}_a; w)} \right) dw \right| < \epsilon.$$

Thus,  $H(p_a)$  is a continuous function of  $p_a$ .

**Lemma 3.3.** Let  $\bar{p}_a$  be a point at which  $f_a(p)$  intersects  $S_{k_+}^+$  and  $\underline{p}_a$  be a point at which  $S_a$  intersects  $S_0^+$ .

- i.  $H(p_a)$  satisfies  $\lim_{p_a \rightarrow \bar{p}_a} H(p_a) = \infty$ .
- ii.  $H(p_a)$  satisfies  $\lim_{p_a \rightarrow \underline{p}_a} H(p_a) = \infty$ .

*Proof.* For part (i), the proof is similar to that of Lemma 2.6 in [5], but requires some changes for the  $g_+(w)$  system and the expression of  $H$  as a function of a point rather than a  $w$  value. The line tangent to  $S_{k_+}^+$  at  $(k_+, 0)$  is  $v = \lambda_{k_+}^-(w - k_+)$ , where  $\lambda_{k_+}^- = \frac{-c - \sqrt{c^2 - 4g'_+(k_+)}}{2}$ . For any small  $\delta > 0$ , there exists some  $w_\delta \in [0, k_+)$  near to  $k_+$  such that the line  $v = (\lambda_{k_+}^- - \delta)(w - k_+)$  is above  $S_{k_+}^+$  for  $w \in (w_\delta, k_+)$ . Let  $T_p$  be an arbitrary trajectory such that  $T_p$  intersects the  $w$ -axis at some  $w_*$  such that  $w_* \in (w_\delta, k_+)$ . Equation (3.1) yields

$$H(p_a) \geq \int_{w_\delta}^{w_*} \frac{1}{v_+^+(p_a; w)} dw \geq \int_{w_\delta}^{w_*} \frac{1}{(\lambda_{k_+}^- - \delta)(w - k_+)} dw, \tag{3.7}$$

where the last integral approaches  $\infty$  as  $w^*$  approaches  $k_+$ . Thus,  $H(p_a) \rightarrow \infty$  as  $w^*$  approaches  $k_+$  from the left. Since  $H(p_a)$  depends continuously on  $p_a$ ,  $w^* \rightarrow k_+$  as  $p_a \rightarrow \bar{p}_a$ . Therefore,  $H(p_a) \rightarrow \infty$  as  $p_a \rightarrow \bar{p}_a$ .

By arguments in Lemma 2.6 of [5], trajectories near the origin but below  $S_0^+$  can travel arbitrarily large distances in  $x$  for any small distance in  $w$ . Thus, for a fixed  $b$ , there exists some point on  $S_b$  arbitrarily close to  $(0,0)$ . The tangent line to  $S_0^+$  at  $(0,0)$  is  $v = \lambda_0^- w$  where  $\lambda_0^- = \frac{-c - \sqrt{c^2 - 4g'_+(0)}}{2}$ . For any small  $\delta > 0$  with  $\delta < |\lambda_0^-|$ , there exists some  $w_\delta \in (0, a)$  and  $v_\delta < 0$  such that the line  $v = (\lambda_0^- + \delta)w$  is above  $S_0^+$  for  $w \in (0, w_\delta)$ , and  $g_+(w) > (g'(0) - \delta)w$  for  $w \in (0, w_\delta)$ . Let  $T_p$  be an arbitrary trajectory below  $S_0^+$  which is close to  $S_0^-$  near the origin so that  $(w_b, v_b) = T_p|_{x=b}$  has  $w_b < w_\delta$  and  $v_b > v_\delta$ . Equation (2.2) for a trajectory  $v_+^-(p_a; w)$  which is below the  $w$ -axis yields

$$\frac{dv_+^-}{dw} = -c - \frac{g_+(w)}{v_+^-} < 0. \tag{3.8}$$

Consider that  $v_+^-(p_a; w)$  is a decreasing function of  $w$ . Since the line  $v = (\lambda_0^- + \delta)w$  is above  $S_0^+$  which is in turn above  $T_p$  for  $w \in (w_b, w_\delta)$  and  $v \in (v_\delta, v_b)$ , Eqs (3.1) and (3.8) along with a variable change yield

$$\begin{aligned} H(p_a) &\geq \int_{w_b}^{w_\delta} \frac{1}{-v_+^-(p_a; w)} dw \\ &\geq \int_{v_b}^{v_\delta} \frac{1}{v_+^-} \frac{1}{-c - g_+(w)/v_+^-} dv_+^- \\ &\geq \int_{v_b}^{v_\delta} \frac{1}{-cv_+^- - g_+(w)} dv_+^- \end{aligned}$$

$$\begin{aligned} &\geq \int_{v_b}^{v_\delta} \frac{1}{-cv_+^- - (g_+'(0) - \delta)w} dv_+^- \\ &\geq \int_{v_b}^{v_\delta} \frac{1}{\left(-c - \frac{g_+'(0) - \delta}{\lambda_0 + \delta}\right)v_+^-} dv_+^- \end{aligned}$$

As  $v_b \rightarrow 0$ , the final integral approaches  $\infty$ , as does  $H(p_a)$ . Since  $H(p_a)$  depends continuously on  $p_a$ ,  $v_b \rightarrow 0$  as  $p_a \rightarrow \underline{p}_a$ . Thus,  $H(p_a) \rightarrow \infty$  as  $p_a \rightarrow \underline{p}_a$ .

**Lemma 3.4.** Fix  $a$ ,  $b$ , and  $L$  such that  $0 \leq a \leq b \leq L$ .

- i. For  $p$  on  $v - a_0w = 0$ ,  $f_a(p)$  forms a continuous curve that takes values arbitrarily close to the origin and intersects  $S_{k_+}^+$  above the  $w$ -axis.
- ii. For  $p$  on the negative  $v$ -axis,  $f_b(p)$  forms a continuous curve that takes values arbitrarily close to the origin and intersects  $U_{k_+}^+$  below the  $w$ -axis.

*Proof.* By arguments in Lemma 2.3 (ii) and Lemma 2.6 in [5], trajectories in the  $g_-(w)$  system sufficiently near the origin and below  $S_0^+$  can travel any positive fixed distance in  $x$  for any small distance in  $w$  and  $v$ . A similar symmetrical argument above the axis yields the same result for trajectories sufficiently close to the origin and above  $U_0^+$ , and a similar argument to that made in Lemma 2.3 (i) yields the same result for trajectories below  $U_0^+$  in the case that  $a_0 < \mu_0^+$ . Thus, for all  $a$  and  $L - b$ , there exist points on  $f_a(p)$  and  $f_b(p)$  arbitrarily close to the origin regardless of whether the line  $v - a_0w = 0$  is above or below  $U_0^+$  near the origin.

Thus, clearly  $f_a(p)$  is inside  $S_{k_+}^+$  for some  $p$  on  $v - a_0w = 0$ . Suppose  $p^*$  is a point on  $v - a_0w = 0$  but outside  $S_{k_+}^+$ . By Lemma 3.1 the corresponding trajectory cannot cross below  $S_{k_+}^+$  for  $x \leq a$ . Further, by the phase plane analysis, it is known that trajectories outside  $S_{k_+}^+$  do not cross the  $w$ -axis, so that  $f_a(p^*)$  is above the  $w$ -axis. Thus, by the continuity of  $f_a(p)$ ,  $f_a(p)$  must intersect  $S_{k_+}^+$ . This proves statement (i).

By prior arguments  $f_b(p)$  is inside  $U_{k_+}^+$  for some  $p$  on the negative  $v$ -axis. Since the boundary conditions give that trajectories evaluated at  $x = L$  must be on the negative  $v$ -axis, trajectories must be below  $S_0^-$  for  $x > b$ . Thus, since  $S_0^-$  is below the  $w$ -axis, trajectories are below the  $w$ -axis for  $x > b$ . Suppose  $p^*$  is a point on the negative  $v$ -axis below  $U_{k_+}^+$ . By Lemma 3.1, the trajectory corresponding to  $p^*$  could not have been inside  $U_{k_+}^+$  for any  $x \geq b$ . Therefore,  $f_b(p)$  has a point below  $U_{k_+}^+$ , and so by continuity of  $f_b(p)$  in  $p$ ,  $f_b(p)$  intersects  $U_{k_+}^+$ .

Next, we define  $H^*$ , which represents the minimum protection zone size required for species persistence given the sizes of the less inhabitable patches.

For fixed  $a > 0$  and  $L - b > 0$ , define

$$H^* = \inf_{p_a \in D_a} H(p_a), \quad (3.9)$$

where  $H(p_a)$  is given by (3.1).  $H^*$  is well defined by Lemmas 3.2 and 3.3, and  $H^* > 0$ .

The following theorem describes the existence of positive steady-state solutions. A positive steady-state solution is positive in the interval  $(0, L)$ .

**Theorem 3.1.** Assume Hypotheses 2.1 hold. Fix  $a > 0$  and  $L - b > 0$ . Then, for  $H^*$  as defined by (3.9):

- i. If  $b - a = H^*$ , systems (1.1)–(1.2) with (1.3) have a positive steady-state solution;
- ii. If  $b - a > H^*$ , systems (1.1)–(1.2) with (1.3) have at least two positive steady-state solutions;
- iii. If  $H^* > 0$  and  $b - a < H^*$ , systems (1.1)–(1.2) with (1.3) have no positive steady-state solution.

*Proof.* Lemmas 2.3 and 2.4 give that  $H^*$  occurs for some  $p_a \in S_a$ . Thus, a corresponding solution exists for  $b - a = H^*$ . When  $b - a > H^*$ , there exists at least two points  $p_a^1, p_a^2 \in S_a$  such that  $H(p_a^1) = H(p_a^2) = b - a$ . Consequently, there exist at least two positive steady-state solutions when  $b - a > H^*$ . For a positive solution to exist, there must be some  $p_a \in S_a$  such that  $b - a = H(p_a)$ . Therefore, if  $b - a < H^*$ , which is defined as the infimum of  $b - a$  values, there exists no positive steady-state solution.

#### 4. Simulations

In this section, we further explore the dynamics of the model through numerical simulations. We first consider

$$g_+(u) = w(1.5 - w)(w - 0.2), \quad g_-(u) = w(1 - w)(w - 0.7), \quad a_0 = 2, \quad (4.1)$$

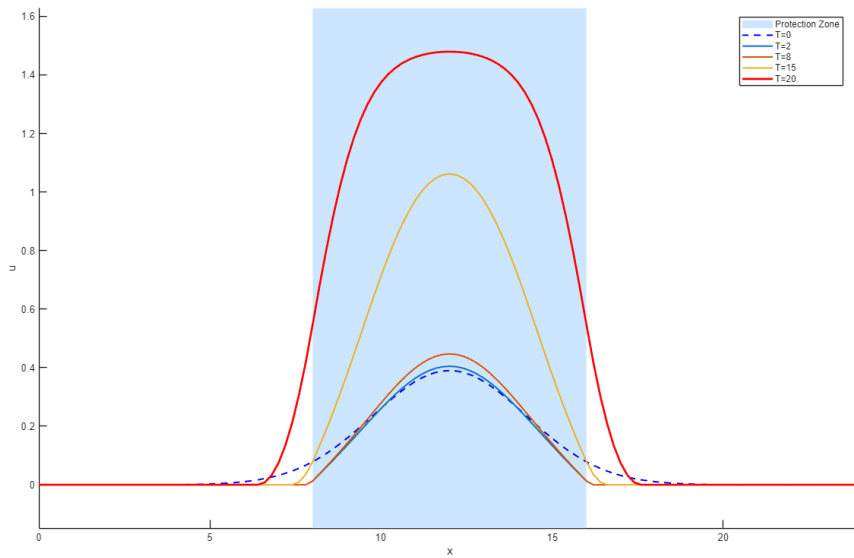
and

$$a = 8, \quad b = 16, \quad L = 24. \quad (4.2)$$

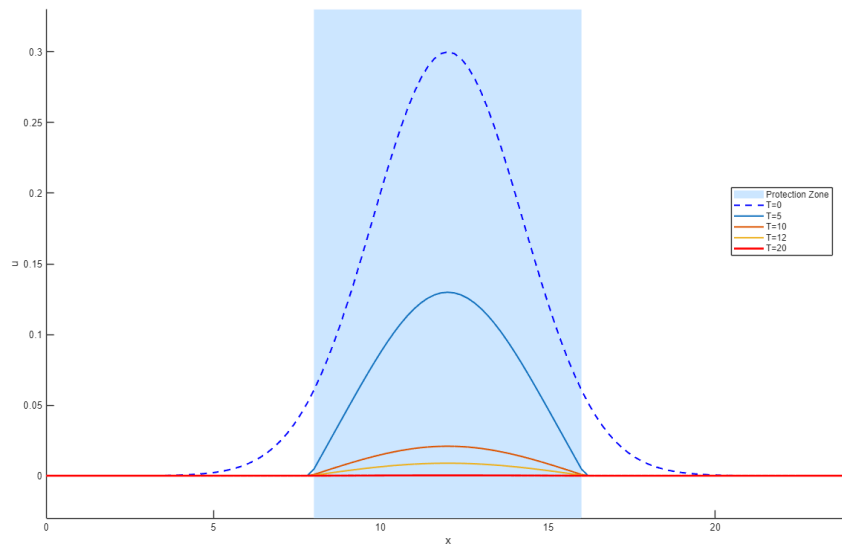
Figure 6 illustrates the population dynamics of the model with (4.1)–(4.2),  $c = 0$ , and different initial data. In this case,  $H^* = 4.179$ , so that  $b - a = 8 > H^*$ , and the model admits multiple positive steady-state solutions.

Figure 7 shows the population dynamics of the model with (4.1)–(4.2),  $c = 0.2$ , and different initial data. In this case,  $H^* = 4.380$ , so that  $b - a = 8 > H^*$ , and the model again admits multiple positive steady-state solutions.

Figures 6 and 7 suggest that population persistence depends sensitively on the initial condition. We conjecture that, in general, when  $b - a > H^*$ , the model admits two positive steady-state solutions, with the larger one being stable and the smaller one unstable. Notably, the initial condition  $u_0(x) = 0.39e^{-0.1(x-12)^2}$  leads to population persistence when  $c = 0$  (see Figure 6), but results in population extinction when  $c = 0.2$  (see Figure 7). This indicates that increasing  $c$  makes population persistence more difficult.



(a)



(b)

**Figure 6.** Evolution of solutions with different initial conditions for the model with (4.1)–(4.2) and  $c = 0$ . (a) The solution with initial condition  $u_0(x) = 0.39e^{-0.1(x-12)^2}$  converges to a positive steady state. (b) The solution with  $u_0(x) = 0.3e^{-0.1(x-12)^2}$  converges to zero.

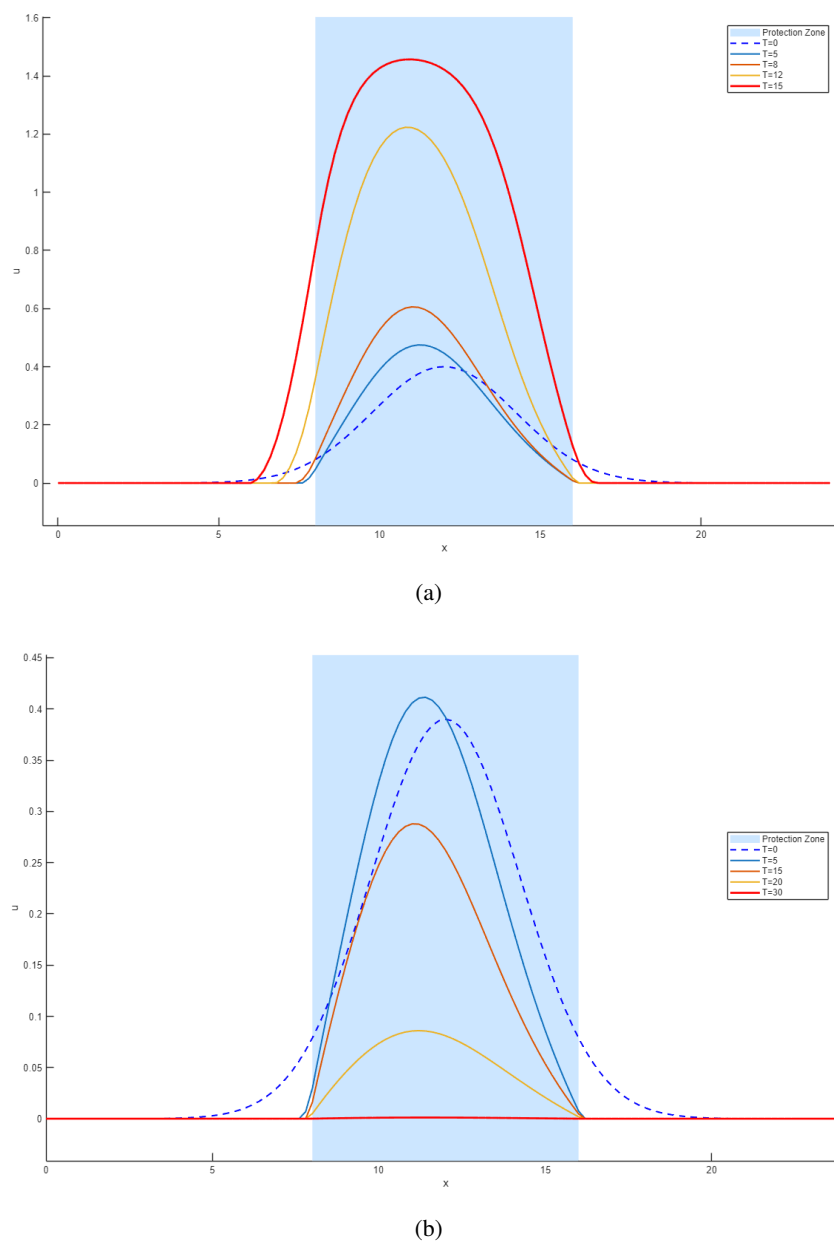


**Figure 7.** Evolution of solutions with different initial conditions for the model with (4.1)–(4.2) and  $c = 0.2$ . (a) The solution with initial condition  $u_0(x) = 0.4e^{-0.1(x-12)^2}$  converges to a positive steady state. (b) The solution with  $u_0(x) = 0.39e^{-0.1(x-12)^2}$  converges to zero.

Next, Figure 8 demonstrates that for sufficiently large  $c$ , the population becomes extinct even when the initial condition is  $u_0(x) \equiv k_+$ . This suggests that, for large  $c$ , the population is unable to keep pace with habitat movement and consequently goes extinct.

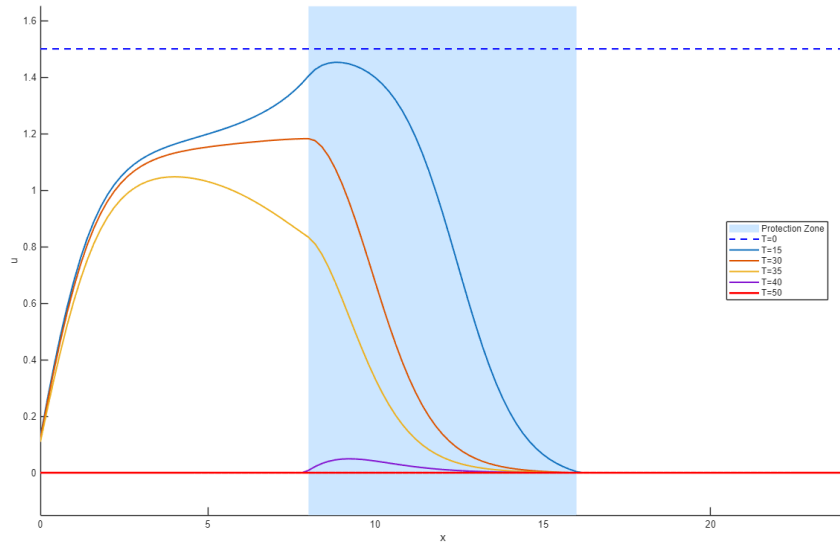


**Figure 8.** Evolution of the solution with  $u_0(x) \equiv k_+$  for the model with (4.1)–(4.2) and  $c = 1$ . The solution converges to zero.

The minimal protection zone size  $H^*$  plays a critical role in determining population persistence. Figure 9 illustrates the dependence of  $H^*$  on  $c$ . Here, the model satisfies (4.1) with  $a = 8$  and  $L - b = 8$ , while the protection zone size  $b - a$  varies.

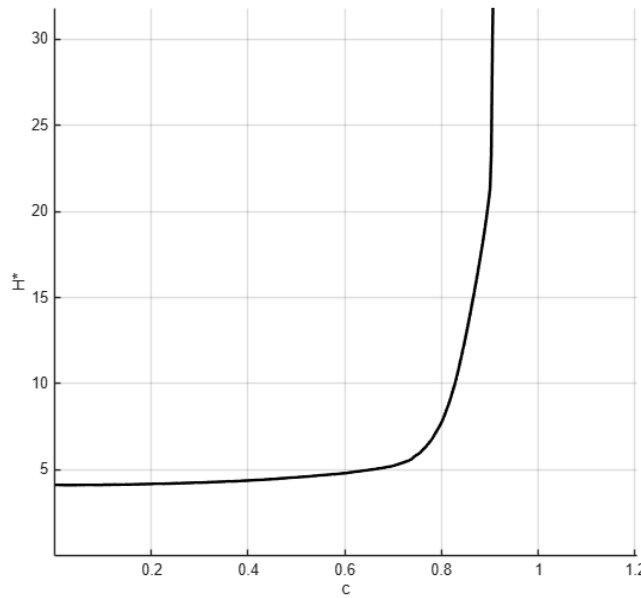


**Figure 9.** Dependence of  $H^*$  on  $c$  for the model with (4.1), where  $a = 8$ ,  $L - b = 8$ , and  $c$  varies.

From Figure 9, we observe the existence of an asymptotic value of  $c$  beyond which population persistence is no longer possible.

Finally, we investigate how  $c$  affects the total population size for the models (4.1)–(4.2) with  $g_+(u)$  replaced by  $w(1.5 - w)(w - 0.3)$ . The total population size is defined as the integral of the stable steady-state solution over the entire habitat  $[0, L]$ . Figure 10 shows that the total population size decreases as  $c$  increases.

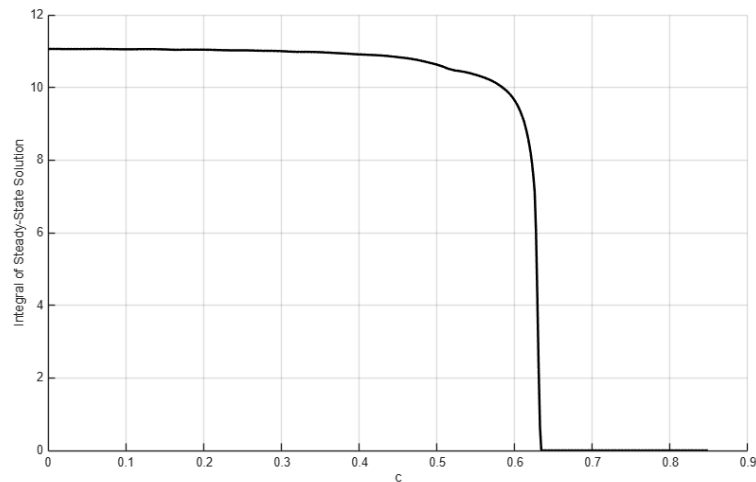


**Figure 10.** Dependence of the total population size on  $c$  for the model with (4.1)–(4.2) with  $g_+(u)$  replaced by  $w(1.5 - w)(w - 0.3)$ .

## 5. Conclusions

In this paper, we studied a reaction–advection–diffusion model describing population dynamics in a heterogeneous habitat composed of a protection zone and outer patches, incorporating strong Allee effects. The advection term models biased dispersal, such as the directional movement of species in rivers or streams. The protection zone is governed by a strong Allee effect function  $g_+$ , which has a positive integral and supports species persistence. In contrast, the outer patches are less favorable for survival and are modeled by a strong Allee effect function  $g_-$  with a negative integral.

After formulating the model, we investigated the associated steady-state problem for both Allee functions. Previous work by Li and Otto [5] analyzed the dynamics of the  $g_+$  system, while Johnson studied the  $g_-$  system in the special case  $c = 0$  [22]. Our work extends these results by examining the  $g_-$  system for  $c > 0$  using phase plane methods. We compared the qualitative behaviors of the two systems and analyzed the dynamics of a mixed system incorporating both  $g_+$  and  $g_-$ .

Using phase plane analysis, we identified key regions and invariant curves and expressed the spatial variable  $x$  as an integral along solution trajectories. This formulation enabled us to establish relationships between these curves and the habitat length. In particular, given the sizes of the outer patches, we showed that the required size of the protection zone can be determined. Moreover, as initial conditions approach the stable or unstable manifolds of the  $g_+$  system, the length of the protection zone tends to infinity. We also established the existence of positive steady-state solutions for sufficiently large protection zones, depending on the size of the outer patches.

The quantity  $H^*$  plays a central role in determining the minimal size of the protection zone required for species persistence. When the size of the protection zone exceeds  $H^*$ , the system admits at least

two positive steady-state solutions. Numerical simulations presented in Section 5 show that population persistence or extinction depends sensitively on the initial data. When the protection zone size is larger than  $H^*$ , relatively large initial data lead to persistence, whereas small initial data result in extinction. These simulations suggest that the model may admit a stable positive steady-state solution that characterizes the long-term population behavior. Furthermore, the numerical results indicate that population persistence becomes more difficult as the advection speed increases, and that both  $H^*$  and the total long-term population size decrease as the advection speed increases.

Despite these findings, several important questions remain open. Although Theorem 3.1 guarantees the existence of solutions for sufficiently large habitat lengths, it is not yet known whether multiple solutions exist at the minimal habitat length, or how many solutions may exist for larger lengths. In addition, the stability properties of positive steady-state solutions have not been analytically established. Moreover, the dependence of population dynamics on parameters other than the advection speed was not explored in this work. We leave these problems for future investigation.

Our phase plane analysis focused on a region in the  $(w, v)$ -plane bounded by the line  $v = a_0 w$  and the negative half of the  $v$ -axis, corresponding to the boundary conditions  $u_x = a_0 u$  at  $x = 0$  and  $u = 0$  at  $x = L$  given in (1.3). For more general boundary conditions of the form

$$\alpha_1 u_x - \beta_1 u = 0 \quad \text{at } x = 0, \quad \alpha_2 u_x - \beta_2 u = 0 \quad \text{at } x = L,$$

the approach developed in this paper remains applicable for analyzing steady-state solutions. In this case, the phase plane region is bounded by two lines determined by the boundary conditions and by the stable and unstable manifolds of the system. While changes in boundary conditions alter the bounding lines, the stable and unstable manifolds remain unchanged. It would be of interest to investigate how boundary conditions influence  $H^*$ , the minimal domain size required for population persistence.

Finally, the model incorporates a piecewise-defined growth function to represent environments with patchy spatial structure, where different regions support different population dynamics. In particular, when considering a barrier zone, the framework allows for alternative configurations—such as strong Allee effects in the outer patches and a less hospitable region in the center—which can be analyzed using similar methods.

## Acknowledgments

B. Li was partially supported by the National Science Foundation under Grants DMS-1951482 and DMS-2451240. The authors thank the referees for their valuable comments and suggestions, which have led to significant improvements to the paper.

## Conflict of interest

The authors declare no conflict of interest.

## Use of AI tools declaration

The authors declare no artificial intelligence (AI) tools used in the preparation of this manuscript.

## References

1. K. Du, R. Peng, N. Sun, The role of protection zone on species spreading governed by a reaction–diffusion model with strong Allee effect, *J. Differ. Equ.*, **266** (2019), 7327–7356. <https://doi.org/10.1016/j.jde.2018.11.035>
2. Y. Du, J. Shi, A diffusive predator–prey model with a protection zone, *J. Differ. Equ.*, **229** (2006), 63–91. <https://doi.org/10.1016/j.jde.2006.01.013>
3. K. P. Hadeler, F. Rothe, Travelling fronts in nonlinear diffusion equations, *J. Math. Biol.*, **2** (1975), 251–263. <https://doi.org/10.1007/BF00277154>
4. Y. Jin, R. Peng, J. Wang, Enhancing population persistence by a protection zone in a reaction–diffusion model with strong Allee effect, *Physica D: Nonlinear Phenom.*, **454** (2023), 133840. <https://doi.org/10.1016/j.physd.2023.133840>
5. B. Li, G. Otto, Forced traveling waves in a reaction–diffusion equation with strong Allee effect and shifting habitat, *Bull. Math. Biol.*, **85** (2023), 121. <https://doi.org/10.1007/s11538-023-01221-9>
6. Y. Lou, F. Lutscher, Evolution of dispersal in open advective environments, *J. Math. Biol.*, **69** (2014), 1319–1342. <https://doi.org/10.1007/s00285-013-0730-2>
7. L. G. Shoemaker, J. A. Walter, L. A. Gherardi, M. H. DeSiervo, N. I. Wisnoski, Writing mathematical ecology: A guide for authors and readers, *Ecosphere*, **12** (2021), e03701. <https://doi.org/10.1002/ecs2.3701>
8. B. Gallardo, D. C. Aldridge, P. González-Moreno, J. Pergl, M. Pizarro, P. Pyšek, et al., Protected areas offer refuge from invasive species spreading under climate change, *Global Change Biol.*, **23** (2017), 5331–5343. <https://doi.org/10.1111/gcb.13798>
9. R. D. Holt, Spatial heterogeneity, indirect interactions, and the coexistence of prey species, *Am. Nat.*, **124** (1984), 377–406. <https://doi.org/10.1086/284280>
10. M. Jerry, A. Rapaport, P. Cartigny, Can protected areas potentially enlarge viability domains for harvesting management, *Nonlinear Anal.: Real World Appl.*, **11** (2010), 720–734. <https://doi.org/10.1016/j.nonrwa.2009.01.042>
11. J. Ren, J. Chen, C. Xu, J. van de Koppel, M. S. Thomsen, S. Qiu, et al., An invasive species erodes the performance of coastal wetland protected areas, *Sci. Adv.*, **7** (2021). <http://dx.doi.org/10.1126/sciadv.abi8943>
12. X. Xu, A. Huang, E. Belle, P. De Frenne, G. Jia, Protected areas provide thermal buffer against climate change, *Sci. Adv.*, **8** (2022), eabo0119. <http://dx.doi.org/10.1126/sciadv.abo0119>
13. C. Parmesan, Ecological and evolutionary responses to recent climate change, *Annu. Rev. Ecol. Evol. Syst.*, **37** (2006), 637–669. <https://doi.org/10.1146/annurev.ecolsys.37.091305.110100>
14. W. C. Allee, *Principles of Animal Ecology*, Philadelphia, Saunders Co, 1949. <https://doi.org/10.5962/bhl.title.7325>
15. I. M. Parker, Mating patterns and rates of biological invasion, *PNAS*, **101** (2004), 13695–13696. <https://doi.org/10.1073/pnas.040578710>
16. A. Kuparinen, S. U. Heikkilä, Atlantic cod recovery from the Allee effect zone: Contrasting ecological and evolutionary rescue, *Fish Fish.*, **21** (2020), 916–926. <https://doi.org/10.1111/faf.12470>

17. C. J. Mcowen, W. W. L. Cheung, R. R. Rykaczewski, R. A. Watson, L. J. Wood, Is fisheries production within large marine ecosystems determined by bottom-up or top-down forcing, *Fish Fish.*, **16** (2015), 623–632. <https://doi.org/10.1111/faf.12082>
18. P. C. Fife, *Mathematical Aspects of Reacting and Diffusing Systems*, Springer-Verlag, 1979. <https://doi.org/10.1007/978-3-642-93111-6>
19. J. Nagumo, S. Yoshizawa, S. Arimoto, Bistable transmission lines, *IEEE Trans. Circuit Theory*, **12** (1965), 400–412. <https://doi.org/10.1109/TCT.1965.1082476>
20. R. D. Benguria, M. C. Depassier, Speed of fronts of the reaction-diffusion equation, *Phys. Rev. Lett.*, **77** (1996), 1171–1173. <https://doi.org/10.1103/PhysRevLett.77.1171>
21. Y. Kametaka, On the stabilization of solutions of the Cauchy problem for the equations arising in the theory of combustion, *Mat. Sbornik*, **59** (1962), 245–288.
22. I. Johnson, *Effects of a Protection Zone in a Reaction-diffusion Model with Strong Allee Effect*, Ph.D thesis, University of Louisville, 2023. <https://doi.org/10.18297/etd/4216>
23. J. K. Hale, *Ordinary Differential Equations*, Krieger, Malabar, Florida, 1980.



AIMS Press

© 2026 the Author(s), licensee AIMS Press. This is an open access article distributed under the terms of the Creative Commons Attribution License (<http://creativecommons.org/licenses/by/4.0>)